Original Article

The Efficacy of a Scaffold-free Bio 3D Conduit Developed from Autologous Dermal Fibroblasts on Peripheral Nerve Regeneration in a Canine Ulnar Nerve Injury Model: A Preclinical Proof-of-Concept Study

Sadaki Mitsuzawa[1] , Ryosuke Ikeguchi[1], Tomoki Aoyama[2], Hisataka Takeuchi[1], Hirofumi Yurie[1], Hiroki Oda[1], Souichi Ohta[1], Mika Ushimaru[3], Tatsuya Ito[3], Mai Tanaka[2], Yoshihiro Kunitomi[4], Manami Tsuji[4], Shizuka Akieda[4], Koichi Nakayama[5], and Shuichi Matsuda[1]

Abstract

Autologous nerve grafting is widely accepted as the gold standard treatment for segmental nerve defects. To overcome the inevitable disadvantages of the original method, alternative methods such as the tubulization technique have been developed. Several studies have investigated the characteristics of an ideal nerve conduit in terms of supportive cells, scaffolds, growth factors, and vascularity. Previously, we confirmed that biological scaffold-free conduits fabricated from human dermal fibroblasts promote nerve regeneration in a rat sciatic nerve injury model. The purpose of this study is to evaluate the feasibility of biological scaffold-free conduits composed of autologous dermal fibroblasts using a large-animal model. Six male beagle dogs were used in this study. Eight weeks before surgery, dermal fibroblasts were harvested from their groin skin and grown in culture. Bio 3D conduits were assembled from proliferating dermal fibroblasts using a Bio 3D printer. The ulnar nerve in each dog's forelimb was exposed under general anesthesia and sharply cut to create a 5 mm interstump gap, which was bridged by the prepared 8 mm Bio 3D conduit. Ten weeks after surgery, nerve regeneration was investigated. Electrophysiological studies detected compound muscle action potentials (CMAPs) of the hypothenar muscles and motor nerve conduction velocity (MNCV) in all animals. Macroscopic observation showed regenerated ulnar nerves. Low-level hypothenar muscle atrophy was confirmed. Immunohistochemical, histological, and morphometric studies confirmed the existence of many myelinated axons through the Bio 3D conduit. No severe adverse event was reported. Hypothenar muscles were re-innervated by regenerated nerve fibers through the Bio 3D conduit. The scaffold-free Bio 3D conduit fabricated from autologous dermal fibroblasts is effective for nerve regeneration in a canine ulnar nerve injury model. This technology was feasible as a treatment for peripheral nerve injury and segmental nerve defects in a preclinical setting.

Keywords

peripheral nerve injury, scaffold-free, Bio 3D conduit, nerve regeneration, preclinical study, proof of concept

[1] Department of Orthopaedic Surgery, Kyoto University Graduate School of Medicine, Kyoto, Japan
[2] Department of Physical Therapy, Human Health Sciences, Kyoto University Graduate School of Medicine, Kyoto, Japan
[3] Institute for Advancement of Clinical Translational Science, Kyoto University Hospital, Kyoto, Japan
[4] Cyfuse Biomedical K.K., Tokyo, Japan
[5] Department of Regenerative Medicine and Biomedical Engineering Faculty of Medicine, Saga University, Saga, Japan

Corresponding Author:
Ryosuke Ikeguchi, Department of Orthopaedic Surgery, Kyoto University Graduate School of Medicine, 54 Shogoin Kawahara-cho, Sakyo-ku, Kyoto 8507, Japan.
Email: ikeguchir@me.com

Introduction

Direct tensionless end-to-end nerve repair achieves the most promising outcomes for neurotmesis. It is widely accepted that interposed autologous nerve grafting is the gold standard for segmental nerve defects when tensionless direct repair cannot be performed[1,2]. In autologous nerve grafting, unlike heart, liver, kidney, or lung transplantation, the engrafted tissue does not itself function as a replacement tissue; rather, it offers a scaffold for axonal elongation. Yet autologous nerve grafting has several potential disadvantages, including donor site morbidity, risk of neuroma formation, mismatch of caliber diameter, limited availability, necessity of extra surgical incisions, increased operative time, and elevated cost[3]. Nerve allograft, which overcomes some of these disadvantages, requires a perioperative immunosuppression and a particular preservation method[4]; because this procedure is intended to correct merely non-life-threatening sensory and motor disturbance, the appropriateness of using systemic immunosuppression therapy for this purpose remains controversial.

The tubulization technique with artificial nerve conduit represents a possible alternative method for nerve autograft and allograft and is already used in selected clinical settings[5]. In association with the development of tissue engineering, several studies have investigated the characteristics of an ideal nerve conduit in terms of its supportive cells, scaffolds, growth factors, and vascularity. Being artificial materials, however, these conduits retain the insuperable problems of low biocompatibility, foreign body reaction, and risk of infection.

To address these potential problems, we introduced the novel technology of Bio 3D, a computer-controlled 3D printing system[6]. The nerve conduit that we created using the Bio 3D printer is a scaffold-free tubular tissue consisting entirely of homogenous multicellular spheroids without synthetic material. Our previous study confirmed the efficacy of the Bio 3D conduit in peripheral nerve regeneration[7]. This concept was distinctively different from the other nerve conduits reported to date, and was considered to be a major breakthrough in the field of nerve regeneration. In that study, however, we transplanted Bio 3D conduits composed of human dermal fibroblasts into immunodeficient rodents, which meant that we were working with heterogenous grafts.

The purpose of the present study was to develop a protocol for using a biological scaffold-free conduit that is entirely composed of autologous dermal fibroblasts using a larger-animal model, and to evaluate the feasibility of this method as a treatment for peripheral nerve injury in a preclinical proof-of-concept study. This is the first study to assess the efficacy of a purely autologous Bio 3D conduit for peripheral nerve regeneration.

Materials and Methods

Animals

Six male beagle dogs (9 months old; weighing 8.1–10.0 kg, Nihon Bioresearch Inc., Gifu, Japan) were used in this study.

Each animal was acclimatized before the surgical procedures, housed in a separate cage, and given standard dog food and water three times a day. Ethical Approval is not applicable for this article. All procedures in this study were conducted in accordance with the guidelines of the Animal Research Committee of Kyoto University approved protocols. There are no human subjects in this article and informed consent is not applicable.

Anesthesia

Animals were sedated with subcutaneous injection of 0.1 ml/kg atropine and intravenous administration of 1 mg/kg thiopental for induction. After intubation, general anesthesia was maintained with inhalation of 2% sevoflurane in oxygen.

Bio 3D Conduits

Approximately 8 weeks before surgery, animals were placed in the supine position under general anesthesia, and a piece of the groin skin was harvested. These skin sections were washed with phosphate-buffered saline (PBS) containing added antibiotics, and their subcutaneous fat layers were thoroughly resected. Dermal fibroblast medium consisted of Fibroblast Basal Medium with Fibroblast Growth supplements (FGM-2) (Cat No.CC-3132 (LONZA, Walkersville, MD, USA) and 10% FBS (Cat No.SH30910.03, Hyclone, Logan, UT, USA). Treated skin was immersed in medium containing 1,000 units/ml of dispase II (Cat No.383-02281, Wako Pure Chemical Industries, Osaka, Japan) and incubated for 3 h. The epidermal layers of the skin sections were then removed, and the remaining tissue was chopped into small particles of 2 mm or less and incubated at 37°C in a humidified 5% CO_2 incubator. Dermal fibroblasts were obtained from these particles and cultured to multiply in vitro. Culture medium was replaced every 2–3 days. Dermal fibroblasts in passage 4–5 were used in this study.

Conduits were assembled from canine dermal fibroblasts utilizing a Bio-3D printer (Regenova®, Cyfuse, Tokyo, Japan) as described by Itoh et al[6]. Briefly, after detachment with trypsin, cells were counted and re-suspended at a density of 1×10^5 cells/ml. Of this cell suspension, 100μl was plated into each well of a Low Cell Adhesion 96-well plate (SUMILON PrimeSurface®, Sumitomo Bakelite, Tokyo, Japan). After 48–72 h, cells aggregated to form a globular shape in each well. The diameter of each of these multicellular spheroids was about 550 ± 50 μm. Using a Bio-3D printer, spheroids were aspirated into a fine suction nozzle from the 96-well plate, skewered into a circular needle-array made of stainless steel, and allowed to develop into a tubular structure according to the pre-designed pattern (Fig. 1A, B). Approximately 1 week after this procedure, adjacent spheroids were conglutinated to create the Bio 3D conduit and the needle-array was removed. The obtained Bio 3D conduits were transferred to a perfusion bioreactor, where a silicon tube with a 5 mm external diameter was
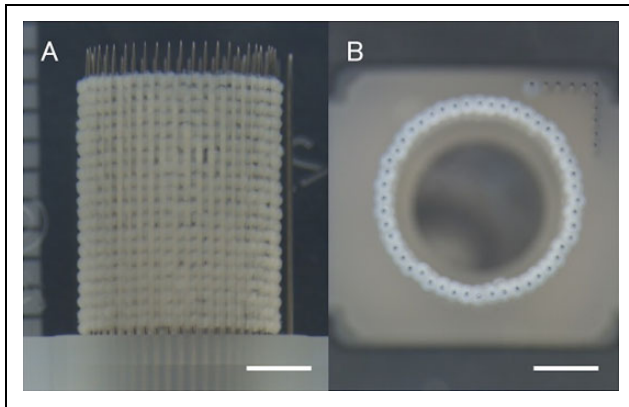
Figure 1. Preparation of the Bio 3D conduit in vitro. Multicellular spheroids were skewered into the circular needle-array according to the pre-designed pattern. (A) viewed from the side, (B) viewed from above. Scale bar: 2 mm.

placed inside each Bio 3D conduit. Perfusion cultivation continued until achieving the desired function and strength (Fig. 2A).

Surgical Technique

Each animal was anesthetized in the supine position and a 5 cm skin incision was made on the volar side of the distal ulnar forelimb. The unilateral ulnar nerve was exposed by retracting the flexor carpi ulnaris medially and the flexor digitorum laterally, and sharply cut at the point 10 mm proximal to the wrist joint. Each dog's own 8 mm Bio 3D conduit was interposed between the proximal and distal stumps. Each stump was then pulled 1.5 mm into the conduit and anchored in place with epineural 9-0 nylon sutures, creating a 5 mm interstump gap in the conduit (Fig. 2B, D). The wound was closed in layers with 4-0 nylon sutures. Following this procedure, a cast was put on the forearm for 2 weeks. All of the postoperative evaluations described below were performed 10 weeks after surgery. The affected ulnar nerves (Bio 3D group) were compared with the unaffected ulnar nerves (Intact group).

Pinprick Test

The pinprick test was performed on the last four animals to evaluate sensory recovery. It could not be performed on the first two animals because of the influence of narcotic drugs. A pinching stimulus was applied by means of standardized forceps from the tip of the fifth digit to the ulnar side of the wrist on the bilateral forearms. Each animal's response to the pinprick test was graded from 0 to 3 as follows: grade 0, no response to stimulus; grade 1, withdrawal response due to stimulus of the ulnar side of the wrist; grade 2, withdrawal response due to stimulus of the fifth metacarpal joint; grade 3, withdrawal response due to stimulus of the tip of the fifth digit.
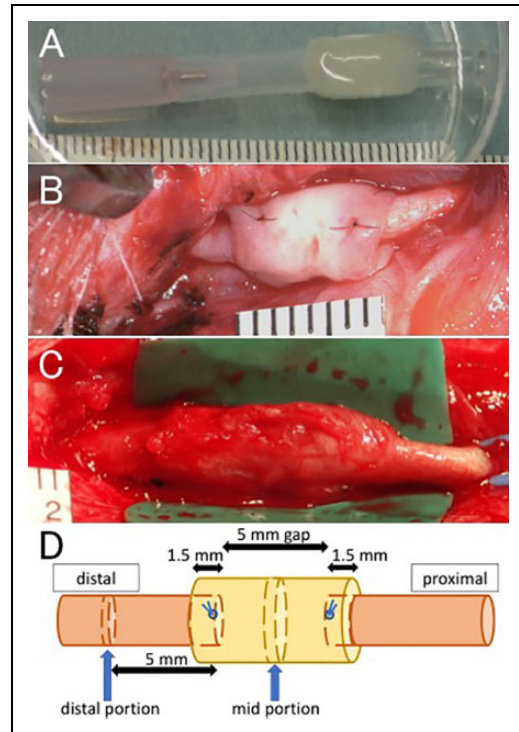

Figure 2. Intraoperative pictures in animal experiments. (A) The obtained Bio 3D conduit after perfusion cultivation just prior to transplantation. (B) An 8-mm Bio 3D conduit was interposed into the nerve defect. The proximal and distal nerve stumps were pulled 1.5 mm into the conduit to create a 5-mm interstump gap. (C) Regenerated ulnar nerve 10 weeks after surgery. The diameter of the Bio 3D conduit remained larger than those of the proximal and distal stumps. (D) In the Bio 3D group, the mid portion of the conduit in the affected ulnar nerve and the distal portion, which is 5 mm distal to the distal sutures, were harvested. In the Intact group, the mid and distal portions of the unaffected ulnar nerve in the same positions were harvested.

Electrophysiological Studies

At 2, 4, 6, and 8 weeks after surgery, under general anesthesia the affected ulnar nerve was stimulated 4 cm proximal to the wrist joint to detect the compound muscle action potentials (CMAPs) of the muscle belly at the base of the ulnarmost digit (hypothenar muscle). Ten weeks after surgery, the bilateral ulnar nerves were exposed under general anesthesia. The affected ulnar nerve was stimulated 4 cm proximal to the wrist joint (S1) and at the wrist joint (S2) with the bipolar silver electrode of an electromyogram measuring system (Neuropack S1, NIHON KOHDEN, Tokyo, Japan). A pair of needle electrodes was inserted into the hypothenar muscle to check for the CMAPs. The amplitude (peak to peak) of the CMAPs that were evoked in the hypothenar muscle with supramaximal electric stimulation from S1 was measured. The accurate distance between S1 and S2 points was measured to calculate the motor nerve conduction velocity (MNCV). The same procedure was performed on the unaffected ulnar nerve.

Macroscopic Observation

Following the electrophysiological study, the position of the Bio 3D conduit was identified from the perineural anchoring sutures at both ends, and the mid portion of the conduit was harvested (Fig. 2C, D). In transverse section, after the boundary between the regenerated nerve and the original conduit was confirmed, the cross-sectional area of regenerated nerve was measured using ImageJ software (National Institutes of Health, Bethesda, MD, USA). The same portion of the unaffected ulnar nerve was harvested, and the cross-sectional area of the intact ulnar nerve was measured using ImageJ software.

Wet Muscle Weight of the Hypothenar Muscle

After nerve samples were harvested, the bilateral hypothenar muscles were exposed and detached from the bone at their origin and insertion, and their wet weights were measured immediately using a digital scale.

Immunohistochemistry

The mid portion of the conduit was harvested from all animals, and fixed with 4% paraformaldehyde (PFA). After cryoprotection with 20% sucrose, transverse frozen sections (18 µm thickness) were prepared. After rinsing with PBS, antigen retrieval was performed using proteinase K (Sigma-Aldrich, St. Louis, MO, USA) at room temperature for 10 min. For blocking, donkey serum was added onto the slides, followed by incubation at room temperature for 1 h. Sections were incubated at 4°C for 24 h with primary antibody, including mouse monoclonal anti-neurofilament H (NF-200) antibody (1:50, Abcam, Tokyo, Japan) and rabbit polyclonal anti-S100 protein (S-100) antibody (1:500, Dako Carpinteria, CA, USA). Slides were then washed with PBS and incubated with secondary antibody [donkey anti-mouse IgG (H+L), CF^{TM} 488 antibody, Sigma-Aldrich; donkey anti-rabbit IgG (H+L), CF^{TM} 543 antibody, Sigma-Aldrich] at room temperature for 1 h. After further PBS washing, cover slips were mounted onto slides using Fluoro-KEEPER Antifade Reagent, Non-Hardening Type with DAPI (Nacalai Tesque Inc., Kyoto, Japan). Slides were viewed using confocal microscopy (BZ-X700; KEYENCE, Osaka, Japan).

Histological and Morphometric Studies

Four nerve samples were harvested from each animal (Fig. 2D): the mid portion of the conduit in the affected ulnar nerve, the distal portion (5 mm distal to the distal sutures in the affected ulnar nerve), and the mid and distal portions of the unaffected ulnar nerve in the same positions. Each nerve sample was fixed in 1% glutaraldehyde and 1.44% PFA, postfixed in 1% osmic acid, and embedded in epoxy resin. Histological and morphometric analysis was performed using ImageJ software, as reported in our previous studies[8–10]. Briefly, transverse sections (1 µm thick) were stained with 0.5% (w/v) toluidine blue solution and examined by light microscopy (ECLIPSE 80i, Nikon, Tokyo, Japan). The total myelinated axon number in the entire neural area in each specimen was calculated at a final magnification of 400×. Ultra-thin sections of the same tissues stained with uranyl acetate and lead citrate were examined using transmission electron microscopy (TEM; Model H-7000, Hitachi High-Technologies, Tokyo, Japan). The shortest diameter of each myelinated axon (a) and bare axon (b) was measured. The mean myelinated axon diameter was expressed as the average value of the shortest diameter of all myelinated axons (a) in seven fields evaluated. The mean myelin thickness was calculated as (a–b)/2 and the G-ratio was calculated as b/a, with each measurement expressed as the average value in seven fields evaluated.

Safety Evaluation

The safety of our scaffold-free Bio 3D conduit transplanting treatment was evaluated by Nihon Bioresearch Inc. (Gifu, Japan). For this safety evaluation, adverse events, clinical signs, body weights, food consumption, urine findings, hematological, and blood chemical findings were assessed, and major organs were examined histopathologically.

Results

Transplantation

All of the conduits were successfully prepared. The average period from skin harvesting to cell suspension into the 96-well plate was 35.8 days. The average period from cell suspension to skewering in the 3D-Bio printer was 2.7 days. The average period from skewering to transplantation was 20.2 days. All five predetermined criteria for the conduits (retaining luminal structure, being easily graspable with forceps, having elastic force, being suitable for needle insertion, and being able to tolerate suturing) were met by all conduits. The size and strength of each conduit was also sufficient to allow it to bridge the 5 mm interstump gap (Fig. 2A).

Pinprick Test

All four unaffected forearms subjected to this test were scored as grade 3. All four affected forearms subjected to this test were also scored as grade 3.

Electrophysiological Studies

The CMAPs of the hypothenar muscles were not present at 2, 4, 6, or 8 weeks after surgery but were detected at 10 weeks after surgery. The mean amplitude of the CMAPs evoked in the hypothenar muscle was 5207 ± 1727 µV in the Intact group, and 388 ± 541 µV in the Bio 3D group. The mean MNCV was 61.1 ± 13.8 m/s in the Intact group, and 34.6 ± 7.0 m/s in the Bio 3D group (Table 1).

Table 1. Summary of Measurement Results.

	Intact group	Bio 3D group
	(N = 6)	(N = 6)
Electrophysiological study		
Amplitude (µV)	5206 ± 1727	388 ± 541
MNCV (m/s)	61.2 ± 13.8	34.6 ± 7.0
Macroscopic observation		
cross-sectional area (mm²)	2.17 ± 0.31	3.34 ± 1.33
Target muscle atrophy		
wet weight of hypothenar muscle (g)	1.12 ± 0.24	0.95 ± 0.14

Macroscopic Observation

The nerve was successfully bridged through the Bio 3D conduit in all animals. The Bio 3D conduits did not fully degrade, however, and remained larger than the proximal and distal stumps (Fig. 2C). In transverse sections, the boundary between the regenerated nerve and the inner wall of the original conduit was readily visible (Fig. 3). The mean cross-sectional area of regenerated nerve was 3.34 ± 1.33 mm² in the Bio 3D group, and the cross-sectional area of the intact ulnar nerve was 2.17 ± 1.33 mm² (Table 1).

Wet Muscle Weight of the Hypothenar Muscle

The mean wet weight of the hypothenar muscle was 1.12 ± 0.25 g in the Intact group and 0.95 ± 0.14 g in the Bio 3D group (Table 1, Fig. 4). These data indicate little muscle atrophy in Bio 3D group because of early reinnervation.

Immunohistochemistry

Immunohistochemical examination revealed NF-200 and S-100 expression in a transverse section of the mid portion of the Bio 3D conduit (Fig. 5). These results indicate the existence of neurofilaments, Schwann cells, and nerve regeneration throughout the Bio 3D conduit.

Histological and Morphometric Studies

In both the mid and distal portions of regenerated nerves, semi-thin toluidine blue-stained transverse sections revealed many well-myelinated axons in the Bio 3D group (Figs 6, 7). In particular, the mid portion of the Bio 3D group exhibited larger numbers of myelinated axons (7066 ± 3169) compared with the Intact group (5744 ± 576), representing axonal sprouting from the proximal nerve stump (Table 2).

Through TEM, the presence of myelinated axons with proper myelin sheaths was confirmed in the Bio 3D group (Table 2), although the post-treatment period of 10 weeks was relatively short and it is possible that thicker myelin formation would have occurred with more time. The distal portions of the nerves in the Bio 3D group showed slightly less mature myelinated axons compared with the proximal portion (Table 3).

Safety Evaluation

No adverse event arose during the postoperative process in any of the six animals with regard to clinical signs, body weights, food consumption, urine findings, hematological and blood chemical findings, or histopathology of major organs (data not shown).

Discussion

The present study demonstrated the efficacy of the Bio 3D conduit and established a protocol for its use in peripheral nerve regeneration. Although the effectiveness of the Bio 3D conduit for peripheral nerve regeneration was confirmed for the first time in our previous report[7], the present study is novel because it involved a larger animal and used each
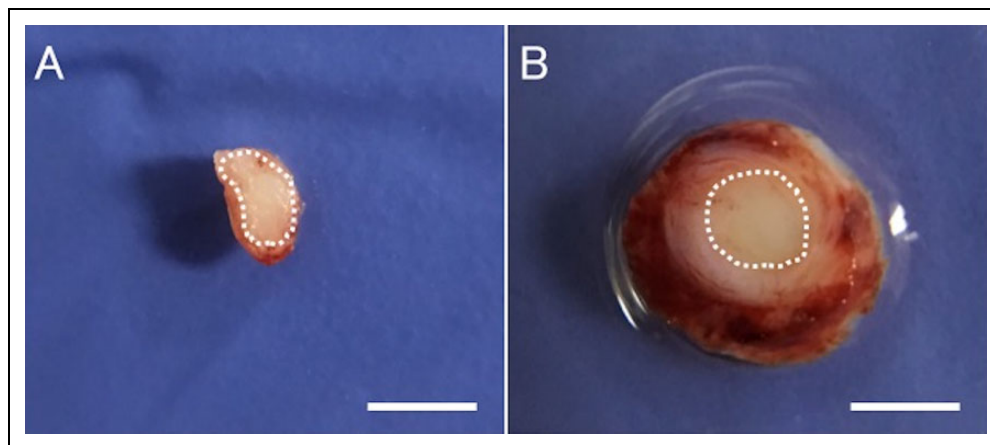

Figure 3. Transverse section of the mid portion. (A) White dotted line represents the cross-sectional area of the intact ulnar nerve. (B) White dotted line represents the boundary between the regenerated nerve and the inner wall of the Bio 3D conduit. Scale bars: 2 mm.
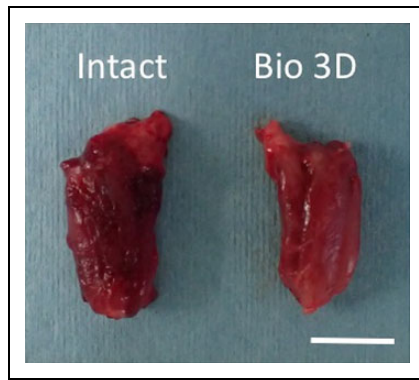
Figure 4. Wet weight of the hypothenar muscle. Little muscle atrophy was observed in Bio 3D group. Scale bar: 10 mm.
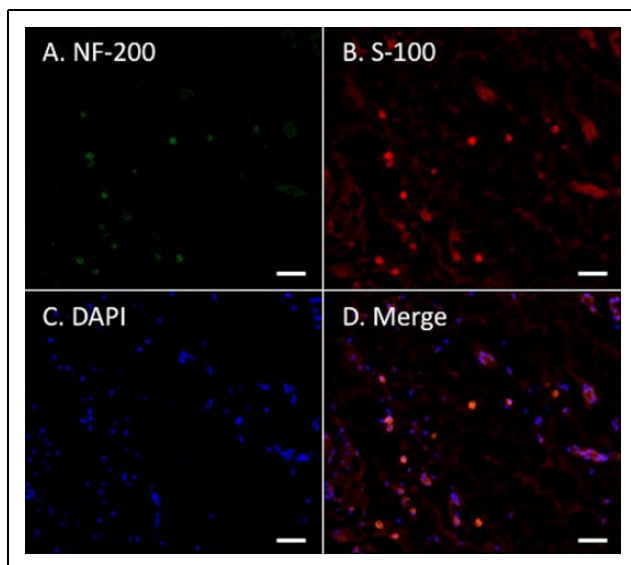

Figure 5. Immunohistochemistry of the mid portion of the Bio 3D conduit. NF-200 and S-100 expression indicate neurofilament and Schwann cells of regenerated nerve at transverse section. Scale bars: 50 μm.

Figure 6. Histological and morphometric evaluation of the mid portions of the intact ulnar nerve and the Bio 3D conduit. (A–D) Semi-thin transverse section (toluidine blue staining) under light microscopy. Scale bars: 1000 μm (A, B) and 50 μm (C, D). (E, F) Ultra-thin transverse section under transmission electron microscopy. Scale bars: 2 μm. Although the myelinated axon diameter in the Bio 3D group is almost the same as that in the Intact group, the myelin thickness in the Bio 3D group is thinner.

animal's cells to generate that animal's conduit. These are important issues for future clinical application.

Various basic researchers have demonstrated that the essential components for nerve regeneration include scaffolds[11–15], vascularity[8–10], supportive cells[16–19], and growth factors[20–23]. In terms of scaffolds, the Bio 3D conduits in the present study were pure biological tissues fabricated from autologous cells so that they would be compatible with surrounding tissues. Eliminating foreign materials diminishes the risk of foreign body reaction, infection, local fibrosis, and allergy, all of which are sometimes triggered by synthetic materials. In addition, the size and length of tubular structures can be freely and adequately designed using a computer system. The wall of a Bio 3D conduit is suffici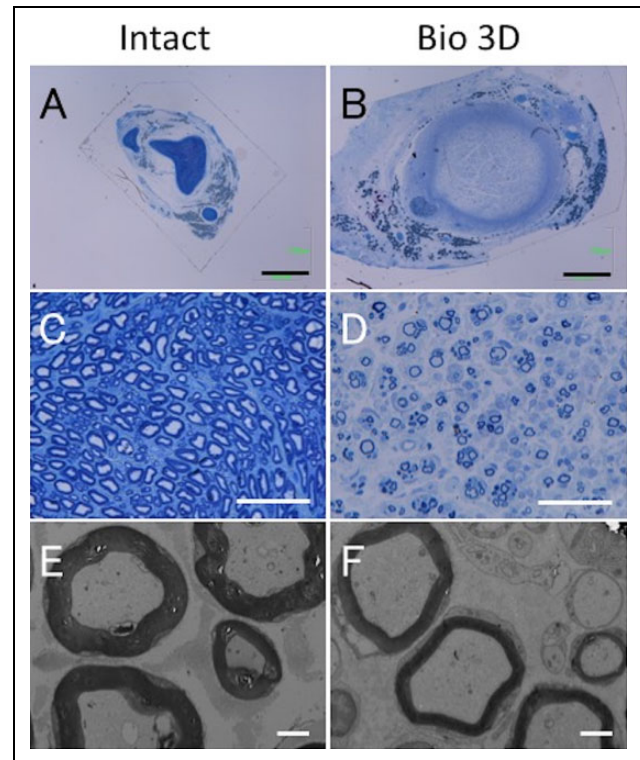ently thick and strong to retain its lumen, hold anchoring sutures, and resist scar formation. From the perspective of vascularity, preinserted vessels inside nerve conduits lead to capillary formation and have been shown to be useful for nerve regeneration. The present study is not in accordance with this strategy. Implanted fibroblasts, however, are less likely to be rejected or to become necrotic and are thus more likely to survive in the original living body. Furthermore, fibroblasts that have been given additional viability through perfusion cultivation before implantation should induce larger amounts of circumferential blood supply compared with artificial materials. From the standpoint of supportive cells, bone marrow stromal cells and adipose-derived stem cells transplanted into the chamber of a conduit have been verified to differentiate into Schwann-like cells which support axonal regeneration. Considering the leakage of implanted cells from conduits and the necessity of cell migration, however, the Bio 3D conduit is capable of bearing far more cells than the nerve conduits can bear, as long as it does not collapse. Neural stem cells are also known to encourage axonal regeneration[24], and are among the strongest candidates for component cells of Bio 3D conduit. Unfortunately, it is difficult to aspirate free-floating
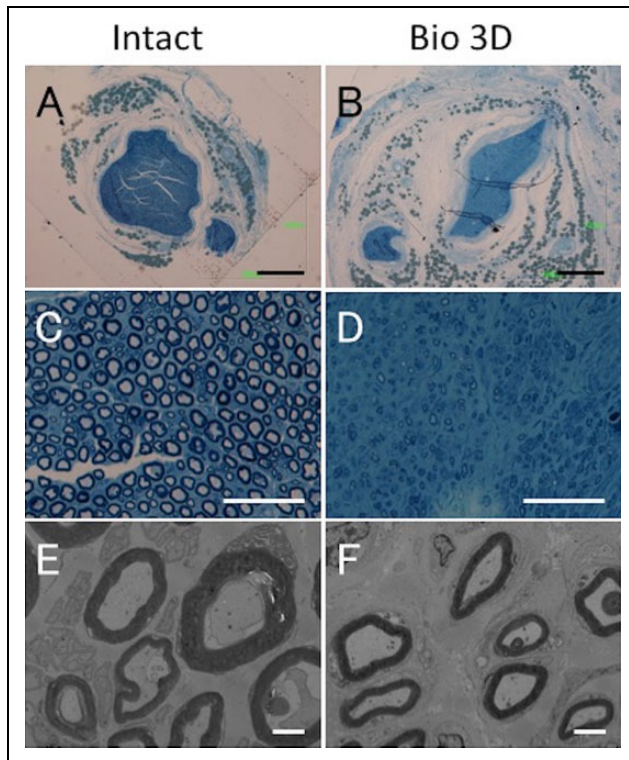
Figure 7. Histological and morphometric evaluation of the distal portions of the intact ulnar nerve and the Bio 3D conduit. (A–D) Semi-thin transverse section (toluidine blue staining) under light microscopy. Scale bars: 500 μm (A, B) and 50 μm (C, D). (E, F) Ultra-thin transverse section under transmission electron microscopy. Scale bars: 2 μm. Although elongated myelinated axons with proper myelin sheaths were confirmed in the Bio 3D group, their morphology was slightly less mature compared with that seen in the distal portion of the Intact group and in the mid portion of the Bio 3D group.

Table 2. Morphometric Studies of the Mid Portions of the Bio 3D Conduit. Larger Numbers of Elongated Myelinated Axons Were Observed Throughout the Bio 3D Conduit, Representing Axonal Sprouting from the Proximal Nerve Stump.

	Intact (mid)	Bio 3D (mid)
Myelinated axon number	5744 ± 576	7066 ± 3169
Myelinated axon diameter (μm)	5.098 ± 0.266	5.462 ± 0.258
Myelin thickness (μm)	1.334 ± 0.127	0.771 ± 0.163
G-ratio	0.462 ± 0.047	0.703 ± 0.055

neurospheres with a suction nozzle, and, once they are skewered into a needle-array, neural stem cells start to differentiate rapidly. For this reason, we did not choose to use neural stem cells to generate the Bio 3D conduit in the present study. Instead, we chose dermal fibroblasts because they are easy to culture and proliferate in vitro, essential for nerve regeneration, and capable of converting into Schwann-like cells[25–27]. So far, co-culture of two different types of cells appears to be superior for nerve regeneration than culture of

Table 3. Morphometric Studies of the Distal Portions of the Bio 3D Conduit. The Distal Portions in the Bio 3D Group Showed Smaller Numbers of Myelinated Axons and Slightly Less Mature Myelin Formation Compared to the Proximal Portions.

	Intact (dist)	Bio 3D (dist)
Myelinated axon number	5649 ± 647	3231 ± 1477
Myelinated axon diameter (μm)	4.495 ± 0.647	3.516 ± 0.613
Myelin thickness (μm)	1.200 ± 0.131	0.707 ± 0.151
G-ratio	0.445 ± 0.051	0.581 ± 0.070

a single cell type[28]. In a mixed spheroid, which consists of two different cell types, the cell distribution changes continuously, and the properties and long-term vitality at the core are improved[29]. By using several spheroids composed of different types of cells, the Bio 3D printer can predesign multiple spheroid layers that mimic the laminar structure of natural neural tissue for future studies. In other studies, various growth factors have been added to the nerve conduit either by being directly injected into the lumen or through one of several alternative delivery systems. Yet loss of quantity through leakage and short-term retention unavoidably make such efforts less effective. This problem could be resolved if the Bio 3D conduit were fabricated from cells that have been genetically modified to overexpress neurotrophic factors[23,30,31]. This is also a point for improvement in future studies.

Scaffold-free tissue has been investigated for clinical use in regenerating cartilage, bone, nerve, skin, blood vessel, and heart muscle[32]. Although several Bio 3D printing technologies for creating tubular tissue have been reported, including the sheet method, the self-aggregation ring method, the cylinder method, and the pulsatile flow/mechanical stimulation method[33–36], we chose to use the recently developed Kenzan method[6,7,37]. This novel technology allows the researcher to design the construction (form, diameter, and length) freely and adequately using a simple computer system. Square needle-arrays have been used for the Kenzan method in previous studies[6,7,37], and our circular needle-array was newly developed for the current study because the form and diameter had already been decided due to other constraints in our experiments. As our robotic skewering system is extremely accurate, the smaller number of needles required also permitted a cost reduction.

The efficacy of the scaffold-free Bio 3D conduit for peripheral nerve regeneration was first reported in our previous study[7]. However, our previous study design in which we transplanted Bio 3D conduits fabricated from human dermal fibroblasts into immunodeficient rodents meant that these were heterogenous grafts. Looking ahead to clinical applications in the future, we prepared the present study using larger animals and transplanting Bio 3D conduits from autologous dermal fibroblasts into the original individuals to attain purely autologous grafts.

We evaluated nerve regeneration by several means. In our electrophysiological studies, all animals demonstrated CMAPs in the hypothenar muscle, although the values of the detected amplitudes and the MNCV varied among individuals. Indeed, the histological and morphometric studies showed many myelinated axons, although our relatively short postoperative period of 10 weeks was not long enough to permit thicker myelination. Longer follow-up periods will enable the accumulation of greater total myelinated axon numbers at the distal portions and the development of thicker myelin sheaths. Macroscopic observations partly differed from those in our previous study[7]. Although the nerve defects were bridged successfully by regenerated nerves in both studies, the process of degradation of the Bio 3D conduit was different. In the rats, the Bio 3D conduits seemed to melt away macroscopically such that the outer diameter of the central portion was almost the same as those of the proximal and distal stumps, making it difficult to identify the boundary line between the original nerve and the Bio 3D conduit without nylon sutures. In the canines, on the other hand, the Bio 3D conduits mostly remained in place, such that both ends could be identified readily. This phenomenon can be explained in terms of immunogenicity. Briefly, transplanted autologous cells are less likely to be rejected or to become necrotic and are more likely to survive in the original individuals. In addition, pure autologous grafts may be presumed to cause less adhesion and inflammatory reaction compared with heterogenous grafts. In transverse sections, the boundary lines between regenerated nerves and the inner walls of the Bio 3D conduits could be accurately detected due to the survival of the Bio 3D conduit. This suggests that we must take great care in determining the internal diameter of each Bio 3D conduit during the computer design programming and perfusion cultivation stages, because a diameter that is too large could cause misdirection (inconsistent topography inside the conduit), while a diameter that is too small could cause entrapment neuropathy. The small degree of atrophy of the hypothenar muscle suggested that the target muscle was re-innervated with regenerated nerves from an early stage.

Although there have been few studies to date on the treatment of human peripheral nerve injury with scaffolds and supportive cells[38,39], our strategy would be suitable for such clinical applications. The period from skin harvest to transplantation required 8 weeks in the current study. Elective surgery would allow enough time to generate a Bio 3D conduit. In emergency situations such as trauma, however, this protocol would not be suitable. Advance preparation for Bio 3D conduit generation from HLA-matched induced pluripotent stem cells might solve this problem in the future.

There are several limitations associated with the present study. First, we did not perform a control study with a nerve autograft or a synthetic material such as a silicone tube. The newly developed Bio 3D conduit should be examined by comparison with the existing method of treatment. One factor obstructing sufficient comparison studies is that only a limited number of large animal species can be used in such experiments, as opposed to the large number of available small animal species. Furthermore, the neuralgic pain inherent to our experiments and the necessity of a postoperative forearm cast led us to use a small sample of canines and to perform the surgical procedure only on unilateral forearms, for the sake of animal welfare. Because a regenerated nerve after a short follow-up period will necessarily be inferior to an intact nerve, statistical analysis was not performed in this study.

Second, we are not entirely sure of how far the axons regenerated distal to the Bio 3D conduit. Once the ulnar nerve was cut, Wallerian degeneration occurred distal to the site of injury and ultimately resulted in myelin tube collapse. Although immunohistochemistry of the distal portion was not performed, toluidine blue staining and TEM revealed the newly elongated axons with proper myelin sheaths at the distal portion, the total count of which reached up to 58% of the mid portion in the Bio 3D group and up to 57% of the distal portion of the Intact group. However, their morphology was slightly less mature compared with that seen in the distal portion of the Intact group. Based on the results of the pinprick test, sensory fibers of regenerated ulnar nerves might reach the tip of the fifth digit. In addition, motor fibers of regenerated ulnar nerves might reach the hypothenar muscle as the target muscle according to the electrophysiological study. To review these data comprehensively, we would suggest that the newly elongated axons and sensory and motor fibers reach the target organs.

Third, our experimental design involved a fairly small interstump gap of 5 mm, which is not critical in canines, and a relatively short follow-up period, as 10 weeks is not enough time to achieve motor functional recovery given the size of our animals. However, this is the first feasibility study to confirm the efficacy of pure autologous Bio 3D conduits in large animals, and we regard the finding of reliable nerve regeneration over a short gap as more important than a less reliable result over a longer and more challenging gap. Once a nerve has begun to regenerate through the Bio 3D conduit, increasing functional recovery can be expected with the passage of time.

Fourth, regarding behavioral analysis, gait analysis was not performed and only a pinprick test for sensory recovery was conducted. Gait analysis may be a better means of assessing motor function. In clinical settings, however, even nerve autografts given according to the gold standard treatment require long follow-up periods of several years to achieve the optimal outcome. Recovery of motor function could hardly be expected after a short follow-up lasting only 10 weeks as in this study. Moreover, although some gait analyses of canines have been reported in recent years, most of these were performed on large dogs, and limited information is available regarding gait analysis in small dogs such as beagles. As gait analysis data differ between dog species, the lack of an established method for beagle gait analysis prevents us from attempting it here. In the present study,

with regard to motor function, reinnervation of the hypothenar muscle was checked by amplitude and MNCV through electrophysiological study.

Fifth, we cannot exclude the possibility that our data regarding the muscle atrophy of the hypothenar muscle were inaccurate. In a rat sciatic nerve injury model, 6-week-old rats more than doubled their body weight and muscle mass during a follow-up period of 8 or 10 weeks. Thus the denervation of the tibialis anterior muscle during this growth period represents muscle atrophy. In the present study, however, the body weight and muscle mass of the 9-month-old dogs remained nearly the same throughout the follow-up period. In that sense, the wet muscle weight data used in this study might not be truly representative of muscle atrophy. However, the hypothenar muscle was expected to have already been re-innervated based on our comprehensive electrophysiological studies and histological and morphometric studies.

Conclusion

We confirmed proof-of-concept for a biological scaffold-free conduit transplantation treatment composed of autologous dermal fibroblasts as a preclinical study. In the treatment of nerve defects, the Bio 3D conduit is considered to be a useful alternative to autologous nerve grafting. Although further research about this procedure's safety, effectiveness, and cost should be performed before Bio 3D conduits can be applied in clinical settings, this technology is expected to resolve several problems in peripheral nerve injury treatment, including cases with trauma or nerve sacrifice during tumor resection.

References

1. Griffin J, Hogan M, Chhabra B, Deal N. Peripheral nerve repair and reconstruction. J Bone Joint Surg Am. 2013;95(23): 2144–2151.
2. Dahlin L. Techniques of peripheral nerve repair. Scandinavian J Surg. 2008;97(4):310–316.
3. Battiston B, Geuna S, Ferrero M, Tos P. Nerve repair by means of tubulization: literature review and personal clinical experience comparing biological and synthetic conduits for sensory nerve repair. Microsurgery. 2005;25(4):258–267.
4. Mackinnon S, Doolabh V, Novak C, Trulock E. Clinical outcome following nerve allograft transplantation. Plast Reconstr Surg. 2001;107(6):1419–1429.
5. Konofaos P, Halen J. Nerve repair by means of tubulization: past, present, future. J Reconstr Microsurg. 2013;29(3): 149–164.
6. Itoh M, Nakayama K, Noguchi R, Kamohara K, Furukawa K, Uchihashi K, Toda S, Oyama J, Node K, Morita S. Scaffold-free tubular tissues created by a Bio-3D printer undergo remodeling and endothelialization when implanted in rat aortae. Plos One. 2015;10(9):e0136681.
7. Yurie H, Ikeguchi R, Aoyama T, Kaizawa Y, Tajino J, Ohta S, Oda H, Takeuchi H, Akieda S, Nakayama K, Matsuda S, et al. The efficacy of a scaffold-free Bio 3D conduit developed from human fibroblasts on peripheral nerve regeneration in a rat sciatic nerve model. Plos One. 2017;12(2): e0171448.
8. Kakinoki R, Nishijima N, Ueba Y, Oka M, Yamamuro T. Relationship between axonal regeneration and vascularity in

tubulation an experimental study in rats. Neurosci Res. 1995; 23(1):35–45.

9. Kaizawa Y, Kakinoki R, Ikeguchi R, Ohta S, Noguchi T, Takeuchi H, Oda H, Yurie H, Matsuda S. A nerve conduit containing a vascular bundle and implanted with bone marrow stromal cells and decellularized allogenic nerve matrix. Cell Transplant. 2017;26(2):215–228.

10. Yamakawa T, Kakinoki R, Ikeguchi R, Nakayama K, Morimoto Y, Nakamura T. Nerve regeneration promoted in a tube with vascularity containing bone marrow-derived cells. Cell Transplant. 2007;16(8):811–822.

11. Nakamura T, Inada Y, Fukuda S, Yoshitani M, Nakada A, Itoi S, Kanemaru S, Endo K, Shimizu Y. Experimental study on the regeneration of peripheral nerve gaps through a polyglycolic acid–collagen (PGA–collagen) tube. Brain Res. 2004; 1027(1–2):18–29.

12. Hsu S, Lu P, Ni H, Su C. Fabrication and evaluation of micro-grooved polymers as peripheral nerve conduits. Biomed Microdevices. 2007;9(5):665–674.

13. Gamez E, Goto Y, Nagata K, Iwaki T, Sasaki T, Matsuda T. Photofabricated gelatin-based nerve conduits: nerve tissue regeneration potentials. Cell Transplant. 2004;13(5): 549–564.

14. Hsieh S, Chang C, Cheng W, Tseng T, Hsu S. Effect of an epineurial-like biohybrid nerve conduit on nerve regeneration. Cell Transplant. 2016;25(3):559–574.

15. Yao M, Zhou Y, Xue C, Ren H, Wang S, Zhu H, Gu X, Gu X, Gu J. Repair of rat sciatic nerve defects by using allogeneic bone marrow mononuclear cells combined with chitosan/silk fibroin scaffold. Cell Transplant. 2016;25(5):983–993.

16. Santiago L, Alvarez J, Brayfield C, Rubin J, Marra K. Delivery of adipose-derived precursor cells for peripheral nerve repair. Cell Transplant. 2009;18(2):145–158.

17. Yamamoto T, Osako Y, Ito M, Murakami M, Hayashi Y, Horibe H, Iohara K, Takeuchi N, Okui N, Hirata H, Nakayama H, et al. Trophic effects of dental pulp stem cells on schwann cells in peripheral nerve regeneration. Cell Transplant. 2016;25(1): 183–193.

18. Siemionow M, Duggan W, Brzezicki G, Klimczak A, Grykien C, Gatherwright J, Nair D. Peripheral nerve defect repair with epineural tubes supported with bone marrow stromal cells. Ann Plast Surg. 2011;67(1):73–84.

19. Widgerow A, Salibian A, Kohan E, Sartiniferreira T, Afzel H, Tham T, Evans G. "Strategic sequences" in adipose-derived stem cell nerve regeneration. Microsurgery. 2014;34(4): 324–330.

20. Fine E, Decosterd I, PapaloÈõzos M, Zum A, Aebischer P. GDNF and NGF released by synthetic guidance channels support sciatic nerve regeneration across a long gap. European J Neurosci. 2002;15(4):589–601.

21. Midha R, Munro C, Dalton P, Tator C, Shoichet M. Growth factor enhancement of peripheral nerve regeneration through a novel synthetic hydrogel tube. J Neurosurg. 2003;99(3): 555–565.

22. Gordon T. The role of neurotrophic factors in nerve regeneration. Neurosurg Focus. 2009;26(2):E3.

23. Lee A, Yu V, Lowe J, Brenner M, Hunter D, Mackinnon S, Sakiyama-Elbert S. Controlled release of nerve growth factor enhances sciatic nerve regeneration. Exp Neurology. 2003; 184(1):295–303.

24. Tang S, Liao X, Shi B, Qu Y, Huang Z, Lin Q, Guo X, Pei F. The effects of controlled release of neurotrophin-3 from PCLA scaffolds on the survival and neuronal differentiation of transplanted neural stem cells in a rat spinal cord injury model. Plos One. 2014;9(9):e107517.

25. Parrinello S, Napoli I, Ribeiro S, Digby P, Fedorova M, Parkinson D, Doddrell R, Nakayama M, Adams R, Lloyd A. EphB signaling directs peripheral nerve regeneration through Sox2-dependent Schwann cell sorting. Cell. 2010;143(1):145–155.

26. Thoma E, Merkl C, Heckel T, Haab R, Knoflach F, Nowaczyk C, Flint N, Jagasia R, Zoffmann S, Truong H, Petitjean P, et al. Chemical conversion of human fibroblasts into functional Schwann cells. Stem Cell Reports. 2014;3(4):539–547.

27. Sowa Y, Kishida T, Tomita K, Yamamoto K, Numajiri T, Mazda O. Direct conversion of human fibroblasts into Schwann cells that facilitate regeneration of injured peripheral nerve in vivo. Stem Cells Translational Med. 2017;6(4): 1207–1216.

28. Dai L, Huang G, Hsu S. Sciatic nerve regeneration by cocultured Schwann cells and stem cells on microporous nerve conduits. Cell Transplant. 2013;22(11):2029–2039.

29. Moldovan L, Barnard A, Gil C, Lin Y, Grant M, Yoder M, Prasain N, Moldovan N. iPSC-derived vascular cell spheroids as building blocks for scaffold-free biofabrication. Biotechnol J. 2017;12(12):1700444.

30. Zhao Z, Wang Y, Peng J, Ren Z, Zhang L, Guo Q, Xu W, Lu S. Improvement in nerve regeneration through a decellularized nerve graft by supplementation with bone marrow stromal cells in fibrin. Cell Transplant. 2014;23(1):97–110.

31. Meyer C, Wrobel S, Raimondo S, Rochkind S, Heimann C, Shahar A, Polat O, Geuna S, Grothe C, Talini K. Peripheral nerve regeneration through hydrogel-enriched chitosan conduits containing engineered Schwann cells for drug delivery. Cell Transplant. 2016;25(1):159–182.

32. Demirbag B, Huri P, Kose G, Buyuksungur A, Hasirci V. Advanced cell therapies with and without scaffolds. Biotechnol J. 2011;6(12):1437–1453.

33. L'heureux N, Paquet S, Labbe R, Germain L, Auger F. A completely biological tissue-engineered human blood vessel. FASEB J. 1998;12(1):47–56.

34. Luo J, Qin L, Kural M, Schwan J, Li X, Bartulos O, Cong X, Ren Y, Gui L, Li G, Ellis M, et al. Vascular smooth muscle cells derived from inbred swine induced pluripotent stem cells for vascular tissue engineering. Biomaterials. 2017;147: 116–132.

35. Norotte C, Marga F, Niklason L, Forgacs G. Scaffold-free vascular tissue engineering using bioprinting. Biomaterials. 2009;30(30):5910–5917.

36. Kelm J, Lorber V, Snedeker J, Schmidt D, Tenzer A, Weisstanner M, Odermatt B, Mol A, Zund G, Hoerstrup S. A novel concept for scaffold-free vessel tissue engineering: self-

assembly of microtissue building blocks. J Biotechnol. 2010; 148(1):46–55.

37. Moldovan N, Hibino N, Nakayama K. Principles of the Kenzan method for robotic cell spheroid-based three-dimensional bio-printing. Tissue Eng. 2017;23(3):237–244.

38. Grimoldi N, Colleoni F, Tiberio F, Vetrano I, Cappellari A, Costa A, Belicchi M, Razini P, Giordano R, Spagnoli D, Pluderi M, et al. Stem cell salvage of injured peripheral nerve. Cell Transplant. 2015;24(2):213–222.

39. Levi A, Burks S, Anderson K, Dididze M, Khan A, Dietrich D. The use of autologous Schwann cells to supplement sciatic nerve repair with a large gap: first in human experience. Cell Transplant. 2016;25(7): 1395–1403.